

# Studying luminal A and B subtypes of breast cancer under paracrine secretion of fibro-blasts

Nazila Jalilzadeh<sup>1,2</sup>, Neda Barzgar Barough<sup>1,3</sup>, Mehrdad Karami<sup>1,3</sup>, Amir Baghbanzadeh<sup>1</sup>, Kobra Velaei<sup>1,3\*</sup>

<sup>1</sup>Immunology Research Center, Tabriz University of Medical Sciences, Tabriz, Iran

<sup>2</sup>Department of Biochemistry, Faculty of Natural Sciences, University of Tabriz, Tabriz, Iran

<sup>3</sup>Department of Anatomical Sciences, Faculty of Medicine, Tabriz University of Medical Sciences, Tabriz, Iran

## Article Info



### Article Type:

Original Article

### Article History:

Received: 17 Sep. 2022

Revised: 4 Apr. 2023

Accepted: 4 Apr. 2023

ePublished: 11 Oct. 2023

### Keywords:

Subtype,  
Breast cancer,  
Tumor microenvironment,  
Cancer-associated  
fibroblast

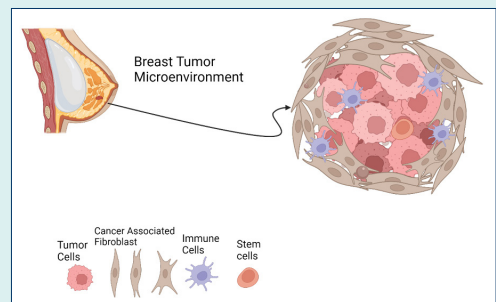
## Abstract

**Introduction:** Understanding the key role of the tumor microenvironment in specifying molecular markers of breast cancer subtypes is of a high importance in diagnosis and treatment. Therefore, the possibility of interconversion of luminal states and their specific markers alteration under the control of tumor microenvironment (TME), particularly cancer-associated fibroblasts (CAFs) deserves to be further investigated.

**Methods:** To activate normal human fibroblasts, liquid overlay technique or nemosis was used and  $\alpha$ -SMA protein expression, CAFs marker, in fibroblastic spheroids was measured by blotting. The luminal A, MCF-7, and luminal B, MDA-MB 361, cell lines were treated with normal and spheroidal/activated fibroblast conditioned medium for 48 hours. The morphological changes of both luminal A and B cells were evaluated by invert light microscopy and analyzed through the shape factor formula. Moreover, chemo-sensitivity, proliferation, and changes in ER-related and proliferative genes expression levels were assessed respectively via MTT assay, Ki67 expression Immunofluorescence assay, real time PCR and Annexin V-FITC techniques.

**Results:** Activated (spheroidal) fibroblasts, expressed  $\alpha$ SMA marker two folds more than monolayer cultured fibroblasts. Our study indicated a significant increase in  $IC_{50}$  of both luminal A and B cell lines after being treated with conditioned medium particularly in treated group with spheroidal conditioned medium. Studying Morphological changes using shape factor formula demonstrated more aggressiveness with gaining mesenchymal features in both luminal A and B subtypes by increasing exposure time. Changes in the expression of Ki67 were observed following treatment with fibroblastic and spheroidal paracrine secretome. Driven Data from Ki67 assay supports the luminal A and B interconversion by elevated Ki67 expression in luminal A and lowered Ki67 expression in luminal B. Gene expression analysis revealed that anti-apoptotic Bcl2 gene expression in both luminal types treated with condition medium has been increased though there has seen no interchange in expression of ER-related and proliferative genes between luminal A (MCF7) and luminal B (MDA-MB361) subtypes, the results of Annexin V-FITC flow cytometry test indicated a decrease in the population of both early and late apoptotic cells in groups treated with both fibroblastic and spheroidal condition medium compared to of control group.

**Conclusion:** Under the paracrine influence of fibroblast cells, both luminal A (MCF7) and luminal B (MDA-MB) subtypes of breast cancer gained invasive, anti-apoptotic, and chemoresistance features which are mostly increased by activated(spheroidal) fibroblasts conditioned medium mimicking CAFs. There was no strong proof for interconversion of luminal A and luminal B which share more similarities among breast cancer molecular subtypes.



\*Corresponding author: Kobra Velaei, Email: [kobraelaei@gmail.com](mailto:kobraelaei@gmail.com)



© 2024 The Author(s). This work is published by BioImpacts as an open access article distributed under the terms of the Creative Commons Attribution Non-Commercial License (<http://creativecommons.org/licenses/by-nc/4.0/>). Non-commercial uses of the work are permitted, provided the original work is properly cited.

## Introduction

Cancer is the second leading cause of death and breast cancer, with a higher prevalence in women, accounts for 29% of cancers and 14% of deaths in women.<sup>1-3</sup> Breast cancer is recognized by heterogeneity, which makes diagnosis, treatment, and prognosis more complex.<sup>4,5</sup> Rudolph Carl Virchow, known as the father of modern pathology, addressed tumor heterogeneity in the early nineteenth century.<sup>6,7</sup>

Breast cancers based on the origin of the cancer cells can be divided into; carcinomas and sarcomas. Carcinomas, the dominant type, are originated from the breast epithelial cells. Sarcomas only comprise less than 1% of breast cancers with the origin of stromal components.<sup>8</sup> In clinic, breast cancer is classified into four molecular subtypes based on hormone receptor expression profile which definitely affects prognosis of malignancy and patient outcome. Luminal A, luminal B, triple-negative, and HER2 enriched are four molecular subtypes of breast cancer.<sup>9,10</sup> Among breast cancer subtypes, Luminal states share more similarities rather than triple-negative and HER2 states. Luminal A includes PR+ (progesterone receptor), ER+ (Estrogen receptor), and HER2- (Human epidermal growth factor receptor 2). Luminal A with the highest incidence (71%), is indicated by lower invasiveness and proliferation rate (Ki67 <14%) along with a satisfying response to hormone therapy.<sup>11,12</sup> Luminal B is PR+, ER+, HER2-/+ which is more aggressive than luminal A (Ki67 ≥ 14%) and comprises 12 % of breast cancers.<sup>13,14</sup>

Non-cancerous part of solid tumors composed of stromal cells such as fibroblasts, immune cells, adipocytes, and mesenchymal stem cells as well as non-cellular components which altogether are named tumor microenvironment (TME).<sup>15-18</sup> According to soil and seed theory, TME as soil and cancer cells as seeds, actively participate in the onset, progression, and metastasis of tumors. On the other hand, mutual interaction between heterogeneous cancer cells and various components of the TME furthers the complexity of breast cancer subtyping.<sup>19,20</sup> Within TME, cancer-associated fibroblasts (CAFs) have been introduced to have a critical role in defining breast cancer subtypes due to dominant position in the TME. Activated CAFs, are characterized by the expression of  $\alpha$ -smooth muscle actin ( $\alpha$ -SMA) which is usually expressed in response to some soluble signaling molecules in TME.<sup>3,18,21,22</sup> The activated fibroblasts crosstalk with tumor cells in multilayers stands for tumor-promotion, and subtyping. However, it was proved that the conversion of basal-like to hormone receptor-positive subtypes occurs through the interaction of platelet-derived growth factor (PDGF)-CC on cancer cells and cognate receptors on CAFs.<sup>20</sup> Therefore interconversion of luminal states or their specific marker alteration under the influence of TME especially CAFs deserves to be more scrutinized.

In this study, we tried to shed more light on CAFs role in

the alteration and/or interconversion of specific markers of breast cancer subtypes. For this purpose, the normal and activated fibroblasts conditioned medium were utilized to simulate the co-culture setting of luminal A and B subtypes which share more similar molecular markers compared to basal-like and HER2 enriched subtypes.

## Methods and Materials

### Materials

Thiazolyl Blue Tetrazolium Blue (MTT) (M2128) powder was purchased from Sigma-Aldrich (St. Louis, MO, USA). Fetal Bovine Serum (FBS), Trypsin/EDTA 0.25% (1726653), and Dulbecco's Modified Eagle's medium (DMEM) (1791923), Roswell Park Memorial Institute Medium were obtained from Gibco (Maryland, USA). RNA isolation kit and primer sequences were obtained from CinnaGen (9561071; Tehran, Iran). The cDNA (AK5601) synthesis kit and PrimeScript RT Master Mix (A9104- 1) were provided by TaKaRa (Tokyo, Japan). Annexin V-FITC apoptosis detection kit was purchased from Immunostep.

### Cell lines and culture

The MCF-7, MDA-MB 361, and HFFF-2 cell lines were purchased from Iran National Cell Bank (Pasteur Institute, Tehran, Iran). Breast cancer cell lines were cultured at 37°C in 5% (v/v) CO<sub>2</sub> using RPMI-1640 medium supplemented with 10% heat-inactivated fetal FBS (Gibco). As well the HFFF-2 fibroblast cell line was cultured using DMEM medium supplemented with 10% heat-inactivated fetal FBS (Gibco).

### Fibroblasts spheroid formation assay (Nemosis)

Firstly, each well of a 6-well plate was coated with 1mL autoclaved agarose gel %1 in PBS to produce a non-adherent surface. Then 10<sup>6</sup> cells/mL were seeded on agarose-coated wells. After 24 hours, spheroids were observed and assessed under invert light microscopy. Furthermore,  $\alpha$ -SMA expression, as an activated fibroblasts marker, in spheroids was measured by western blotting assay.<sup>23</sup> To prepare conditioned medium out of activated fibroblasts(spheroids), the spheroids were cultured with DMEM medium for 48 hours.

### Cell viability assessment using MTT assay

Conditioned medium-treated luminal A (MCF-7) and luminal B (MB-MDA361) cells were seeded in triplicate into flat-bottom 96-well plates (104 cells per well) and treated with different doses of doxorubicin (10, 100, 250, 500, 750, 1000 and 1500 nM). Also, untreated cells served as a control. After incubation for 48 hours with different doses of doxorubicin, cell viability was analyzed using colorimetric methyl thiazol tetrazolium bromide (MTT) assay. After 48 hours, 200  $\mu$ L of 5 mg/mL MTT solution was added to each well of the 96-well plate, and cells were incubated for 4 hours at 37 °C. Eventually, the OD of

samples were read at 570 nm through an ELISA reader following solubilizing formazan crystals by DMSO.

#### **Annexin V-FITC flow cytometry Assay for studying apoptosis**

To evaluate apoptosis, luminal A (MCF-7) and luminal B (MB-MDA 361) cells were seeded in flat-bottom 12 well plates at a density of  $2.0 \times 10^5$  cells per well in the culture medium. After 24 h of culture, luminal A (MCF-7) and luminal B (MB-MDA 361) cells were treated with control (FBS 10%), FCM (FBS 10%+30% fibroblasts condition medium), SCM (FBS 10%+30% spheroidal condition medium), DOX (FBS 10%+ 0.57  $\mu$ M DOX), DOX+FCM (FBS 10%+30% fibroblasts condition medium+ 0.57  $\mu$ M DOX), DOX+SCM (FBS 10%+30% spheroidal condition medium+ 0.57  $\mu$ M DOX), for 48 h. Then the cells were trypsinized, collected and centrifuged to remove the supernatant. The collected cells were rinsed one more time with chilled PBS to eliminate trypsin completely. Then  $5 \times 10^5$  number of cells were suspended in 200  $\mu$ L Annexin binding Buffer. To stain apoptotic cells, Immunostep FITC/Annexin-V apoptosis detection kit was used based on the manufacturer's protocol, which is described as follows: 200  $\mu$ L of cell suspension in BB, 5  $\mu$ L FITC/Annexin-V were incubated for 15 minutes then the samples were centrifuged for removing unbounded Annexin, 200  $\mu$ L of cells suspension in BB were incubated with 2.5  $\mu$ L PI (Propidium Iodide, provided in kit) for 10 more minutes and eventually 500  $\mu$ L of PBS were added to each suspension. Unstained and control-stained groups prepared as well. All samples were read by BD FACSCalibur flow cytometry to analyze apoptotic cells.

#### **Evaluation of the morphological changes in luminal A and B breast cancer cells**

To evaluate the morphological changes in the breast cancer cell lines, the images of cells were captured by inverted light microscope (Optika, Italy). Then, Image J software was used to measure the area and perimeter of the cells. In the next step, the shape factor formula was utilized to evaluate morphological changes (Shape factor =  $4\pi A/P^2$  where A indicates area and P indicates the perimeter of the cells).<sup>24</sup> when the value of Shape factor formula becomes 1 it indicates round epithelial cells (roundness of cells) and when this quantity approaches to zero it indicates mesenchymal cells (elongated cells).

#### **Assessment of mRNA expression level by real time RT-PCR**

The total RNA of samples was extracted using the CinnaGen TRI-ZOL mixture (9561071; Tehran, Iran) according to the manufacturer's protocol. Following extraction, the RNA concentration and purity were assessed using Thermo Fisher's spectrophotometer (Thermo Fisher Scientific Life Sciences, USA) Nano-Drop in 260 nm and 280 nm wavelengths absorbance. Then,

RT PCR technique was employed to assess the changing in the expression of proliferative, CCNE-1, and NESP-1 genes, and ER-related Fox-A and Bcl-2 genes. The cDNA (AK5601) synthesis kit and PrimeScript RT Master Mix (A9104- 1) were provided by TaKaRa (Tokyo, Japan). StepOnePlus™ Real-Time PCR System was applied to perform RT PCR reactions. Utilized primer sequences are displayed in Table 1. Primers were designed using Oligo7.60 software. Beta-actin house keeping gene was employed as internal control. All of the tests were operated in triplicate, and the results were analyzed with 2-dd Ct formula.

#### **Western blotting analysis**

For evaluating  $\alpha$ -SMA (smooth muscle actin) protein level, 40  $\mu$ g of protein was diluted in loading buffer and then denaturized by placing in boiling water temperature of 100 °C for 5 minutes. The protein lysates were electrophoresed on 30.8% SDS- polyacrylamide (37.5:1 acrylamide/bisacrylamide) gel at 120V for 45 minutes and then electrotransferred to the PVDF (Bio-Rad Laboratories, Hercules, USA) using 120V power for 90 minutes. The PVDF was blocked with 5% skimmed milk and Tween-20 TBST for 75 minutes. The primary rabbit anti-human  $\alpha$ -SMA antibody (sc-53015, 1:200) together with blots were incubated overnight with primary rabbit anti-human  $\alpha$ -SMA antibody (sc-53015, 1:200) at -4 °C. In the next step, blots were washed 3 times in TBST buffer and incubated with mouse anti-rabbit IgG-HRP (sc-2357 2, 1:1000) for 75 minutes at room temperature. After incubation, the blots were washed 3 times in TBST buffer and protein bands were detected by applying enhanced chemiluminescence (ELC) detection system.  $\beta$ -actin (sc-47778, 1: 300) was used as the internal control. Eventually, the ImageJ software was used to quantify the protein expression levels obtained from the GelDoc BioRad system.

#### **Immunofluorescence assay**

In the first step,  $3 \times 10^4$  cells per well were cultured on a coverslip in the six-well plate. Following treatment

**Table 1.** The list and sequence of the primers

Name	Sequence (5' → 3')
B-actin-F	TCCCTGGAGAAGAGCTACG
B-actin-R	GTAGTTTCGTGGATGCCACA
FOXA-1-F	TCTGATTAAGCGCTCTGCC
FOXA-1-R	CCATGAACGTGCCACCAA
BCL2-F	CCTGGGATGACTGAGTACC
BCL2-R	GGCAGCATCATCCACACATA
NESP1-F	GCCGGCTTACCATCTCTACC
NESP1-R	GGTCAACGGGCAAAAAGCAA
CCNE1-F	ATACTTGCTGCTTCGGCCTT
CCNE1-R	TCAGTTTGTAGCTCCCCGTC

with conditioned medium, cells were fixed with paraformaldehyde, then were permeabilized with 0.2% Triton-X100 for 15 minutes at 4 °C and subsequently blocked with BSA at room temperature for 60 minutes. In the presence of 3% BSA, samples were incubated with Primary antibody overnight at 4 °C then visualized by conjugation via Alexa Fluor 568 secondary antibodies. For nuclei staining, cells were stained with media containing DAPI for 15 minutes. Then, images were captured using fluorescent microscopy for each sample and quantified using ImageJ software and CTCF (corrected total cell fluorescence) formula = Integrated Density – (Area of selected cell × Mean fluorescence of background readings).

### Statistical analysis

Nonparametric one-way analysis of variance (ANOVA) was performed with Dennett's test, using the software GraphPad Prism 9.2.0 version. Each experiment was carried out in triplicate and repeated three to four times independently.  $P < 0.05$  was considered significant. All data were expressed as mean  $\pm$  SD.

## Results

### Spheroid formation of fibroblasts by liquid overlay technique (LOT) indicated a high expression level of $\alpha$ -SMA

LOT technique, nemosis, was used to activate fibroblast cells, in order to produce activated fibroblasts mimicking CAFs. After transferring  $10^6$  fibroblast cells on agarose gel in each well of a six-well plate, most cells aggregated

and formed spheres within 6 hours (Fig. 1A). The spheres, reached 200  $\mu$ m in diameter. The 3D arrangement of cells in spheres affects the amount of taken oxygen and other essential nutrients into cells causing fibroblast cells activation. Results Obtained from western blot assay (Fig. 1B) revealed that the expression of  $\alpha$ -SMA protein, as a marker of active fibroblasts, in spheroids (HFFF-2S) increased roughly as twice as that of fibroblasts (HFFF-2) (Fig. 1C) in monolayer culture. This result indicated the success of LOT-inducing active fibroblasts to mimic CAFs phenotype. Taken together, the spheres or 3D culture method by LOT demonstrated more features of fibroblast activation rather than the monolayer or 2D culture in terms of mimicking cancer-associated fibroblasts (CAFs).

### Increased chemoresistance by fibroblast CM (conditioned medium) in both luminal A and B breast cancer subtypes

MTT assay was used to study the response of luminal A and B cells to chemotherapy drug doxorubicin (DOX) after being treated by paracrine secretion of fibroblasts. In luminal A subtype, MCF-7 cell line, the  $IC_{50}$  of fibroblastic conditioned medium (FCM) and spheroidal conditioned medium (SCM) groups have been significantly increased compared to the control group (10% FBS). The  $IC_{50}$  dose of the control group has been 1.7  $\mu$ M, which this value in the FCM and SCM-treated groups has been increased to approximately 3  $\mu$ M. In luminal B, MDA-MB-361, an elevation in  $IC_{50}$  dose has been observed in both CM-treated experiments (Fig. 2B). The recorded  $IC_{50}$  doses were respectively 2.1, 5.9, and 7.2  $\mu$ M for the control,

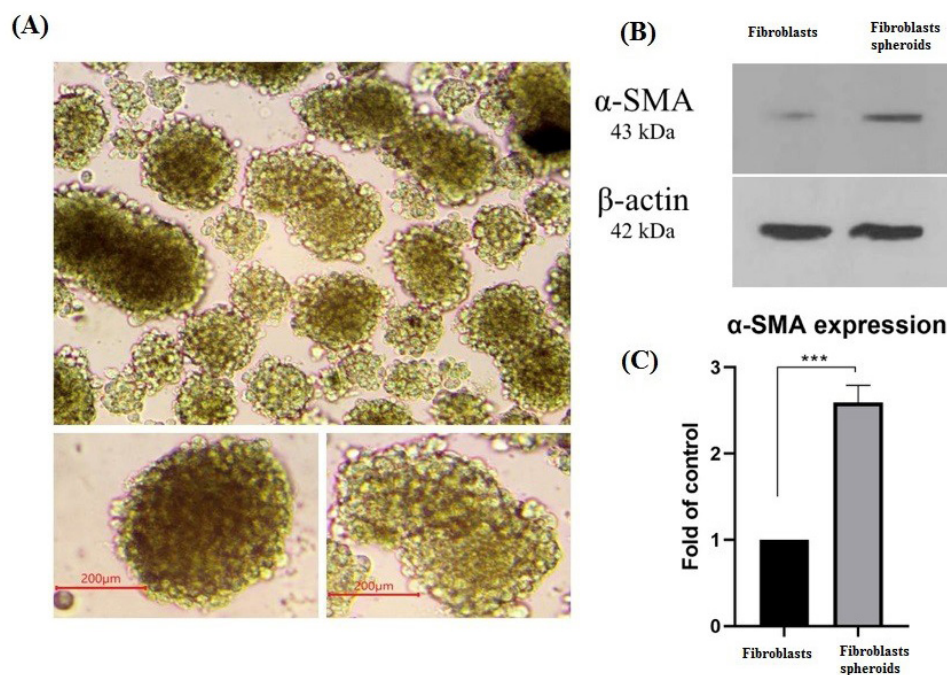


**Fig. 1.**  $\alpha$ -SMA expression indicating activated fibroblasts. (A) fibroblasts 3D cultured (Spheroids) on agarose gel %1 as the non-adhesive surface with 100X magnification. spheroids size on average is more than 200 $\mu$ m (200X), scale bar= 200  $\mu$ m. (B)  $\alpha$ -SMA protein expression in 2D cultured fibroblasts and 3D cultured fibroblasts (spheroids) were evaluated by western blotting,  $\beta$ -actin as housekeeping protein was used as internal control (C) Histogram of  $\alpha$ -SMA protein expression level in 2D cultured fibroblasts and 3D cultured fibroblasts (spheroids). \*\*\* $P \leq 0.001$ .

FCM, and SCM groups (Fig. 2A). Therefore, it can be concluded that due to the conditioning with fibroblastic and spheroidal paracrine secretome the effective cytotoxic dose of the drug (IC<sub>50</sub> value) simultaneously the cell survival rate of both luminal A and B cells have been increased. Though the Decrease in luminal A and B cells chemo-sensitivity to DOX indicates that both subtypes have gained more resistant phenotype to chemotherapeutic agent in the presence of spheroidal and normal fibroblasts secretome, luminal B in comparison to luminal A subtype demonstrated a greater increase in IC<sub>50</sub>, meaning that the paracrine secretome of normal and spheroidal fibroblasts markedly increased the chemoresistance of luminal B cells.

**Anti-apoptotic effect of fibroblastic and spheroidal condition medium has been observed**

Apoptosis of luminal A and B cells under paracrine secretome of normal and spheroidal/activated fibroblasts has been studied, it has been revealed that presence of both fibroblastic and spheroidal condition media caused a decrease in the population of apoptotic cells (Fig. 3A and 3B). Anti-apoptotic effect of FCM and SCM treatment groups has been proved in this section which is inconsistent with obtained data from MTT and real-time PCR experiments.

**Morphological changes of luminal A and B cells under paracrine secretome of normal and spheroidal /activated fibroblasts**

The shape factor formula was used to distinguish the morphological changes in CM-treated cells. A shape factor value for round epithelial cells should be 1 and when this

quantity approaches zero indicates elongated mesenchymal cells. As data shows, a significant decrease in shape factor value was seen after 48 hours in comparison to 24 hours of treatment. The shape factor value for luminal A, MCF-7 cells, in 48 hours fibroblastic conditioned medium (FCM) treated group was 0.55 (Fig. 4A), and this value for luminal B MDA-MB-361 cells was 0.73 (Fig. 4B), showing more cellular elongation compared to the control groups in both MCF-7 and MDA-MB-361 cells. Expectedly spheroidal conditioned medium (SCM) showed a greatest decrease in shape factor value, which means that activated fibroblast paracrine secretion could bring about more mesenchymal features than normal fibroblasts. Therefore, it can be concluded that the secretome of fibroblastic spheroids in the 48 hours exposure time changed the morphology of both luminal A and B cells toward obtaining mesenchymal features which may confer more aggressiveness to both breast cancer subtypes.

**Alteration of Ki67 expression on co-cultured luminal A and B cells with normal and spheroidal/activated conditioned medium**

Given Ki67 as one of the clinical biomarkers in distinguishing luminal A and B subtypes, Immunofluorescence technique was utilized to measure changes in Ki67 expression. Luminal B, MDA-MB-361 cells, expressed higher level of Ki67 in comparison to luminal A, MCF-7 cells. Driven data from MDA-MB 361 cell line demonstrated that the expression of Ki67 decreased in both SCM and FCM-treated groups. The decrease in the SCM group has been statistically significant compared to FCM group (Fig. 5B). Ki67 Expression increased in luminal A MCF-7 cells, in the FCM treated group has also been statistically

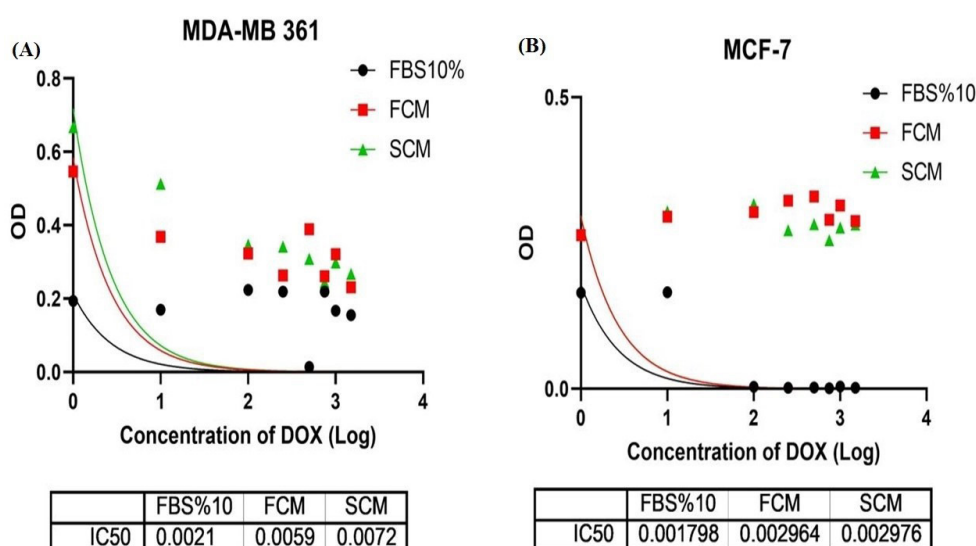


**Fig. 2.** Non-linear regression to calculate best-fit curve of MTT data on luminal A and B. (A) This test has been performed in triplicate with FBS10%, fibroblast conditioned medium (FCM), spheroidal conditioned medium (SCM) groups for 48 hours. Doxorubicin IC<sub>50</sub> in MCF7 cells in FBS 10%, FCM and SCM groups has respectively been 1.7, 2.9 and 2.9 μM. (B) This test has been performed in triplicate with FBS10%, fibroblast conditioned medium (FCM), spheroidal conditioned medium (SCM) groups for 48 hours. Doxorubicin IC<sub>50</sub> in MDA-MB 361 cells in FBS 10%, FCM and SCM groups, has respectively been 2.1, 5.9 and 7.2 μM.

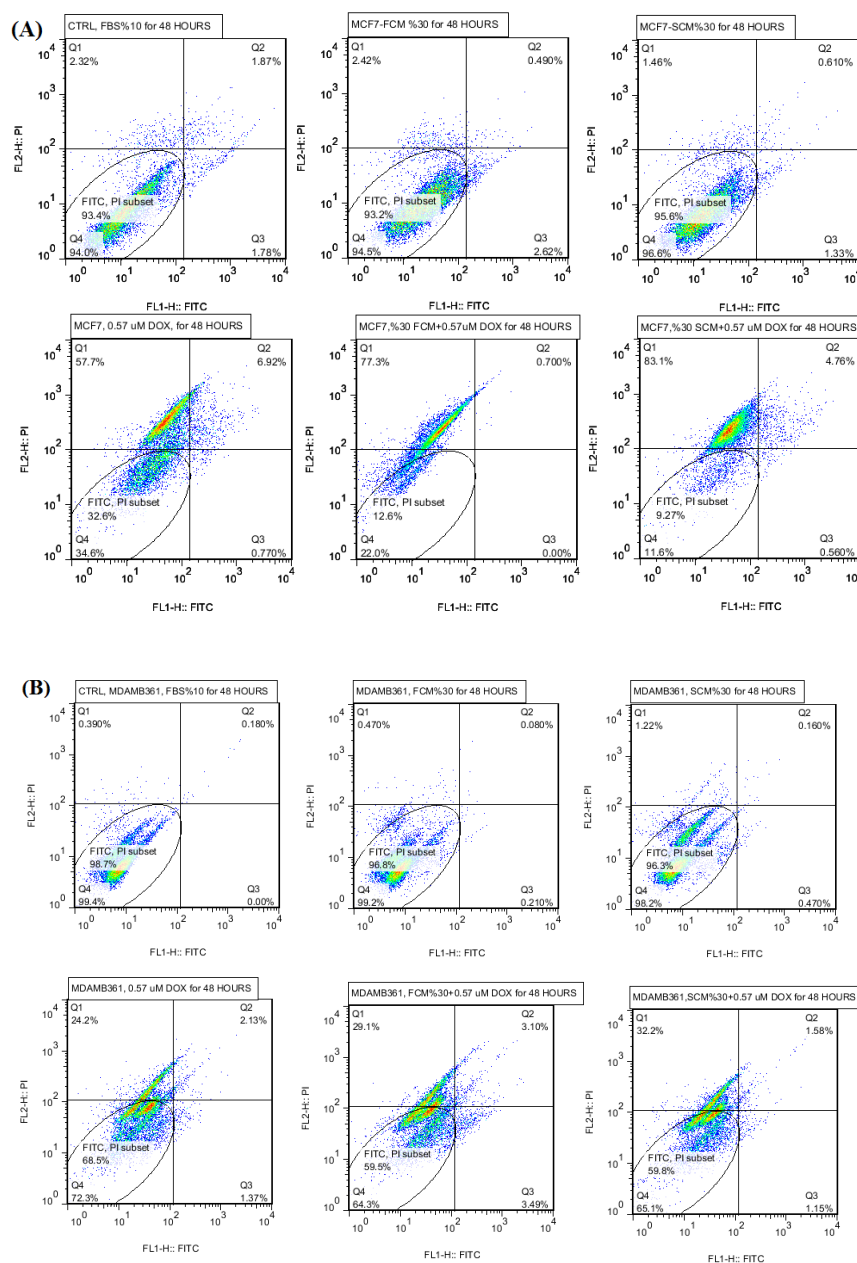


**Fig. 3.** (A) Apoptosis results of luminal A MCF7 cells, treatment groups are including control, FCM, SCM, DOX, FCM+DOX, SCM+DOX. (B) Apoptosis results of luminal B MDAMB361 cells, treatment groups are including control, FCM, SCM, DOX, FCM+DOX, SCM+DOX.

significant. However, significant elevation in the FCM treated group has not been observed. The expression level in this group was the same as in the control group (Fig. 5A). Therefore, in general, it can be concluded that the secretome of normal and activated/spheroidal fibroblasts in both luminal A and B cell lines resulted in changes in the expression of Ki67 indicating probable luminal subtypes phenotype changing under the influence of fibroblasts secretome.

**Expression of proliferative and ER-related genes on luminal A and B Subtypes under influence of activated and normal fibroblast secretome**

The expression of proliferative, CCNE-1, and NESP-1

genes, and ER-related Fox-A and Bcl-2 genes, in luminal A and B subtypes, were evaluated to search for evidence of interconversion of luminal A and B subtypes under the influence of activated and normal fibroblasts paracrine secretome at the mRNA level. It has been proved that ER-related genes were highly expressed in luminal A and proliferative genes pronouncedly expressed in luminal B cells.<sup>25</sup> The results showed that the expression level of proliferative CCNE-1 and NSEP-1 genes, in the presence of CM were decreased in luminal A cells (Fig. 6B). Decreased expression of proliferative genes in luminal B MDA-MB-361 cells has also been observed (Fig. 6B). In general, between estrogen-dependent genes, Bcl-2 was increased in both luminal A and B subtypes (Fig.

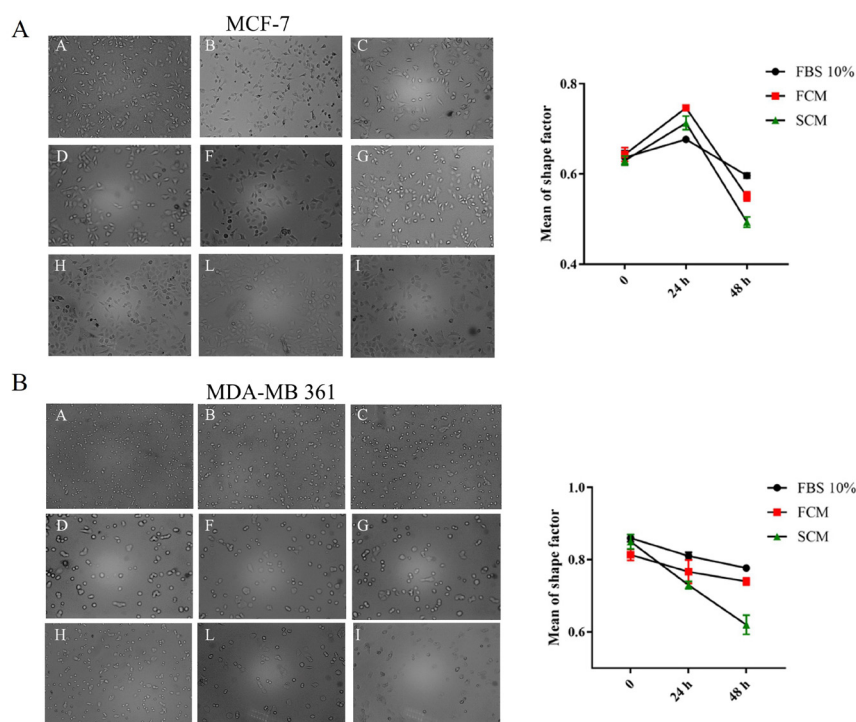


**Fig. 4.** (A) Light microscope images (10X) and linear shape factor value graph of MCF-7 cells. The first row indicates cells treated with FBS 10%, the second row indicates cells treated with fibroblast conditioned medium (FCM), and the third row indicates cells treated with spheroidal conditioned medium (SCM) on 0, 24, and 48 hours of treatment. (B) Light microscope images (10X) and linear shape factor value graph of MDA-MB-361 cells, the first row indicates FBS 10% treated cells, the second row indicates cells treated with normal fibroblast conditioned medium (FCM) and the third row indicates cells treated with spheroidal conditioned medium (SCM) on 0, 24 and 48 hours of treatment.

6A), which indicates the enhancement of anti-apoptotic properties in both luminal subtypes under fibroblasts paracrine secretome. Therefore, any interconversion feature between luminal A and B subtypes of breast cancer cells has not been observed on the mRNA expression level.

## Discussion

Higher incidence rate among women and heterogeneity feature of breast malignancies makes it a tough battle on many fronts.<sup>26</sup> The inevitable interplay between cancer cells and constituents of TME pays to the growth, survival, and heterogeneity of solid tumors in the breast cancer. CAFs as a large and heterogeneous population of stromal cells in breast cancer TME are known by the expression of markers like  $\alpha$ SMA, fibroblast-specific protein 1 (FSP1), and fibroblast activation protein alpha (FAP).<sup>17,27</sup> The experimental in vitro model for activation of fibroblast is nemesis utilizing the liquid overlay technique to produce cell aggregates/spheroids.<sup>28</sup> Hypoxic condition in suspension culture of spheroids mimics the hypoxia of TME in solid tumors which has an essential role in the activation of fibroblasts. Our western blot data revealed that the expression of  $\alpha$ -SMA protein, a marker of activated fibroblasts, in spheroids (fibroblasts spheroids) increased approximately as twice as that of 2D cultured fibroblasts (HFFF-2). This result proved the success of LOT or nemesis, in producing active fibroblasts to simulate CAFs role in TME.<sup>29</sup> Comparison between normal and activated

fibroblasts conditioned medium studied groups revealed that spheroidal fibroblasts in activated state confer much to drug resistance phenotypes, epithelial to mesenchymal transformation, and anti-apoptotic feature compared to normal fibroblasts paracrine secretome in both luminal subtypes.

Based on clinical prognostic factors, genomic status, and immunohistochemical measures adjuvant and neo-adjuvant chemotherapy strategies are suggested in the luminal subtype of breast cancer. However, targeting TME and its major cellular component CAFs to enhance current therapeutic methods is a currently novel idea in clinical policies.<sup>30</sup> CAFs through activation of interferon signaling and collagen/integrin  $\beta$ 1/PI3K/AKT signaling pathways could cause chemo-resistant phenotype.<sup>15,31,32</sup> Our study focusing on the luminal subtypes showed that the resistance to DOX increases in both luminal A and B subtypes which were co-cultured with fibroblast conditioned medium. Compared to luminal A, luminal B cells demonstrated more increase in  $IC_{50}$  of both normal and spheroidal fibroblastic CM treated groups indicating that paracrine secretome of CAFs intensely impacted the response of luminal B subtype to chemotherapy. In lined with driven data from real-time PCR, anti-apoptotic effects in both CM treated group has been observed which it has been more significant in spheroidal condition medium treated group.

In accordance with our results obtained from

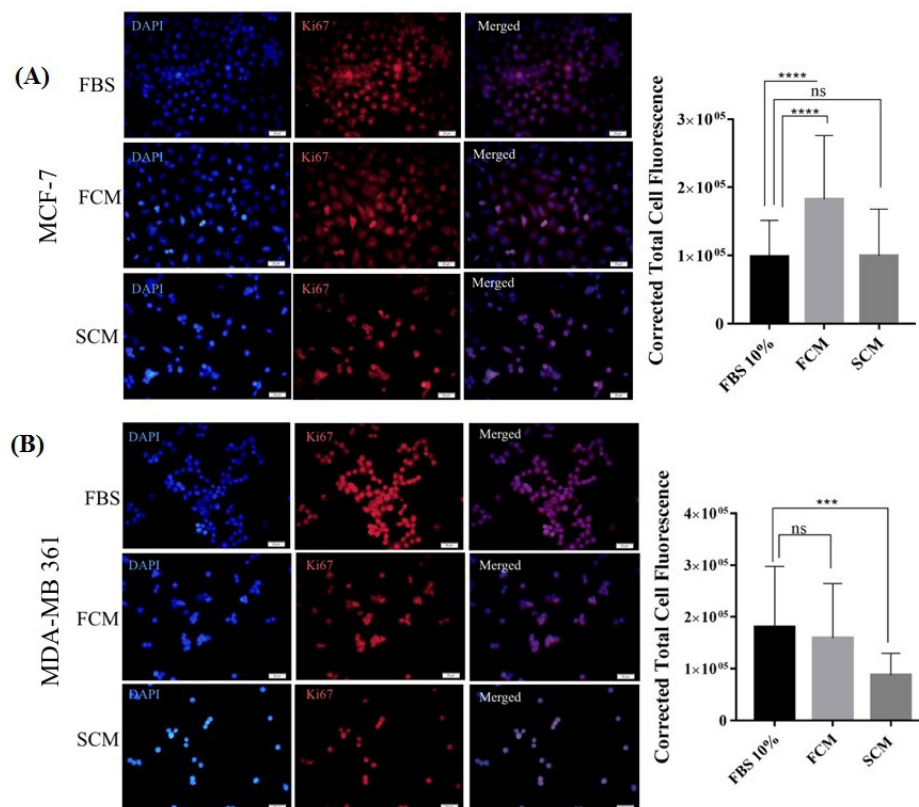


**Fig. 5.** Immunofluorescence microscope images of Ki67 expression in MCF-7 and MDA-MB 361 cells with 400X magnification. (A) The first row indicates MCF-7 cells treated with FBS 10% (control group), the second row indicates cells treated with normal fibroblast conditioned medium (FCM), and the third row indicates cells treated with spheroidal conditioned medium (SCM) for 48 hours. Nuclei are stained with blue DAPI dye. Quantification was performed by ImageJ software through calculating corrected total cell fluorescence (CTCF) and data is presented in a histogram. (B) The first row indicates MDA-MB 361 cells treated with FBS 10% (control group), the second row indicates cells treated with normal fibroblasts conditioned medium (FCM), and the third row indicates cells treated with spheroidal conditioned medium (SCM) for 48 hours. The nuclei were stained with blue DAPI dye. Quantification was performed by image J software through calculating corrected total cell fluorescence (CTCF) and data is presented in a histogram. Scale = 20  $\mu$ M, \*\*\* $P$  ≤ 0.001, non-significant; ns.

morphology assessments, Hu et al on 2019 also reported that, in addition to chemoresistance, CAFs induced epithelial to mesenchymal transition in colorectal cancer cells.<sup>33</sup> Shape factor evaluation with no regard to the luminal type showed that cancer cells tend to get elongated and gain mesenchymal features by increasing the time of treatment with CM to 48 hours. The transition from round epithelial to elongated mesenchymal cells under CAFs influence is an initial step of metastasis. A study on co-culture of CAFs derived exosomes with MCF-7 cells revealed that miR-181d-5p via downregulation of Caudal-related homeobox 2 (CDX2) homeobox A5 (HOXA5) promotes EMT.<sup>33,34</sup> Hence, aggressiveness and migration of luminal A and B subtypes partly depend on their paracrine interplay with stromal cells like CAFs. It seems that gaining an aggressive phenotype in both luminal subtypes lead cells to invasive, basal and undifferentiated states. Subtypes interconversion under the control of TME has been proved with regard to the role of TME in cancer promotion. Based on a study by Roswall et al paracrine crosstalk between platelet-derived growth factor (PDGF)-CC expressing cancer cells and CAFs in basal subtypes of breast cancer could facilitate interconversion of basal

subtypes into the positive hormone receptor subtypes.<sup>20</sup>

Ki67, as a biomarker to distinguish Luminal A and B subtypes, is commonly used for treatment-decision making.<sup>35</sup> Changes in Ki67 expression showed an increasing amount in luminal A compared to luminal B. This data only supports our hypothesis of the possibility of switch between luminal A and B subtypes of breast cancer under influence of fibroblast secretome. However, obtained data from the expression of ER-related genes and proliferative genes in luminal A and B subtypes could not support the luminal A and B phenotypic interconversion/transition. Therefore, it can be concluded that the fibroblasts paracrine secretome only affects Ki67 proliferative marker expression in the luminal A and B subtypes. Moreover, our hypothesis of the interconversion of luminal A and B subtypes under fibroblast influence has not been proven in the mRNA level assessments. The results of gene expression showed that the paracrine secretome of activated and normal fibroblast increased the Bcl2 gene expression level as an anti-apoptotic gene in both luminal A and B subtypes which is in accordance with our data obtained from MTT and flowcytometry. Like our results, a study on CAFs has reported that increased



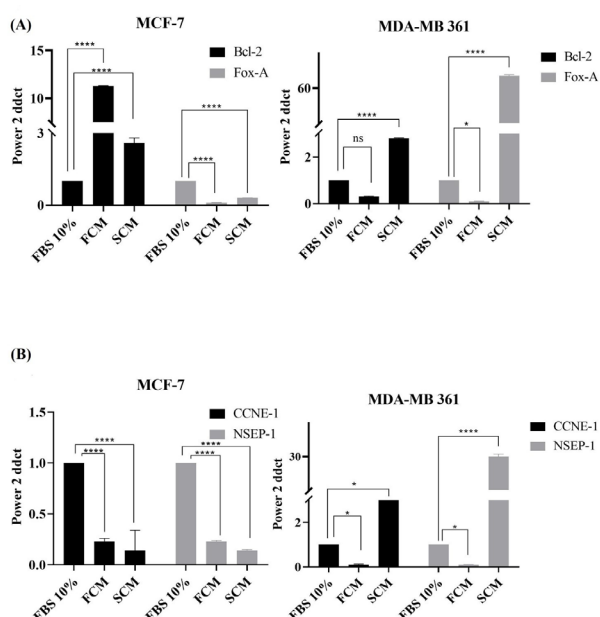


**Fig. 6.** Histograms of ER-related and proliferative genes expression in luminal A and luminal B subtypes. (A) The expression level of ER-related genes, FoxA and Bcl-2, on MCF-7 and MDA-MB 361 cell lines. The control group, FCM, and SCM were treated with Bovine serum 10%, fibroblast conditioned medium, and spheroidal conditioned medium respectively. (B) The expression level of proliferative genes, CCNE-1 and NSEP-1, on MCF-7 and MDA-MB 361 cell lines. The control group, FCM, and SCM were treated with FBS 10%, fibroblast conditioned medium, and spheroidal conditioned medium respectively. The B-actin gene was used as a housekeeping internal control gene, non-significant; ns, \*\*\*\*  $P < 0.0001$ .

IGF-1/ER $\beta$  signaling enhanced chemoresistance and anti-apoptotic rates in bladder cancer cells.<sup>32</sup>

## Conclusion

Under the paracrine influence of fibroblasts, both luminal A and B subtypes of breast cancer gain invasive, anti-apoptotic, and chemoresistance states, markedly increased by activated fibroblast spheroidal) conditioned medium mimicking CAFs. There has been no strong proof for the interconversion of luminal A and B subtypes of breast cancer. Hence, our data support gaining basal-like features with high aggressiveness and resistance to chemotherapy drugs instead of luminal subtypes interconversion.

## Competing Interests

The authors declare that there are no conflicts of interest.

## Ethical Statement

Not applicable.

## Funding

The study has been financially supported by the Immunology Research Center, Tabriz University of Medical Sciences, Tabriz, Iran. This grant supported the MD thesis for Mehrdad Karami (Ethical code: IR.TBZMED.VCR.REC.1400.025, Thesis No:1400/01/30).

## Acknowledgments

The authors thank the Immunology Research Center, Tabriz University of Medical Sciences, Tabriz, Iran for financial and technical support.

## Research Highlights

### What is the current knowledge?

✓ The tumor microenvironment consists of cellular and non-cellular components which their cross-talk is decisive in cancer cell progression, invasion, and metastasis, clarifying the function of these components could provide beneficial knowledge for developing effective cancer diagnosis and therapies.

### What is new here?

✓ The chemoresistance and anti-apoptotic effects of paracrine secretion of activated cancer-associated fibroblasts on both luminal A and B subtypes of breast cancer has been observed.

## Authors' Contribution

**Conceptualization:** Kobra Velaei.

**Data curation:** Nazila Jalilzadeh, Neda Barzegar Barough, Mehrdad Karami, Kobra Velaei.

**Formal analysis:** Nazila Jalilzadeh, Neda Barzegar Barough, Mehrdad Karami, Kobra Velaei.

**Funding acquisition:** Kobra Velaei.

**Investigation:** Nazila Jalilzadeh, Neda Barzegar Barough, Amir Baghbanzadeh, Kobra Velaei.

**Methodology:** Nazila Jalilzadeh, Kobra Velaei.

**Project administration:** Nazila Jalilzadeh, Kobra Velaei.

**Resources:** Kobra Velaei.

**Software:** Kobra Velaei.

**Supervision:** Kobra Velaei.

**Validation:** Kobra Velaei.

**Visualization:** Nazila Jalilzadeh.

**Writing—original draft:** Nazila Jalilzadeh.

**Writing—review & editing:** Nazila Jalilzadeh, Kobra Velaei.

## References

- Fitzmaurice C, Allen C, Barber RM, Barregard L, Bhutta ZA, Brenner H, et al. Global, regional, and national cancer incidence, mortality, years of life lost, years lived with disability, and disability-adjusted life-years for 32 cancer groups, 1990 to 2015: a systematic analysis for the global burden of disease study. *JAMA Oncol* **2017**; 3: 524-548. <https://doi.org/10.1001/jamaoncol.2016.5688>
- Orimo A, Gupta PB, Sgroi DC, Arenzana-Seisdedos F, Delaunay T, Naeem R, et al. Stromal fibroblasts present in invasive human breast carcinomas promote tumor growth and angiogenesis through elevated SDF-1/CXCL12 secretion. *Cell* **2005**; 121: 335-48. <https://doi.org/10.1016/j.cell.2005.02.034>
- Sahai E, Astsaturov I, Cukierman E, DeNardo DG, Egeblad M, Evans RM, et al. A framework for advancing our understanding of cancer-associated fibroblasts. *Nat Rev Cancer* **2020**; 20: 174-186. <https://doi.org/10.1038/s41568-019-0238-1>
- Hyo-eun CB, Ruddy DA, Radhakrishna VK, Caushi JX, Zhao R, Hims MM, et al. Studying clonal dynamics in response to cancer therapy using high-complexity barcoding. *Nat Med* **2015**; 21: 440-8. <https://doi.org/10.1038/nm.3841>
- Datta NR, Samiei M, Bodis S. Radiation therapy infrastructure and human resources in low-and middle-income countries: present status and projections for 2020. *Int J Radiat Oncol Biol Phys* **2014**; 89: 448-57. <https://doi.org/10.1016/j.ijrobp.2014.03.002>
- Beca F, Polyak K. Intratumor heterogeneity in breast cancer. *Adv Exp Med Biol* **2016**; 882: 169-89. [https://doi.org/10.1007/978-3-319-22909-6\\_7](https://doi.org/10.1007/978-3-319-22909-6_7)
- Polyak K. Heterogeneity in breast cancer. *J Clin Invest* **2011**; 121: 3786-8.
- Allred DC. Ductal carcinoma in situ: terminology, classification, and natural history. *J Natl Cancer Inst Monogr* **2010**; 2010: 134-8.

- <https://doi.org/10.1093/jncimonographs/lgg035>
9. Metzger-Filho O, Tutt A, De Azambuja E, Saini KS, Viale G, Loi S, et al. Dissecting the heterogeneity of triple-negative breast cancer. *J Clin Oncol* **2012**; 30:1879-87. <https://doi.org/10.1200/JCO.2011.38.2010>
  10. Dai X, Cheng H, Bai Z, Li J. Breast cancer cell line classification and its relevance with breast tumor subtyping. *J Cancer* **2017**; 8: 3131-3141. <https://doi.org/10.7150/jca.18457>
  11. Dai X, Xiang L, Li T, Bai Z. Cancer hallmarks, biomarkers and breast cancer molecular subtypes. *J Cancer* **2016**; 7: 1281-94. <https://doi.org/10.7150/jca.13141> eCollection 2016.
  12. Mota AdL, Evangelista AF, Macedo T, Oliveira R, Scapulatempo-Neto C, Vieira RAdC, et al. Molecular characterization of breast cancer cell lines by clinical immunohistochemical markers. *Oncol Lett* **2017**; 13: 4708-4712. <https://doi.org/10.3892/ol.2017.6093>
  13. Huelsken J, Hanahan D. A subset of cancer-associated fibroblasts determines therapy resistance. *Cell* **2018**; 172: 643-4. *Cell* **2018**; 172: 643-644. <https://doi.org/10.1016/j.cell.2018.01.028>
  14. Soliman NA, Yussif SM. Ki-67 as a prognostic marker according to breast cancer molecular subtype. *Cancer biology & medicine* **2016**; 13: 496. *Cancer Biol Med* **2016**; 13: 496-504. <https://doi.org/10.20892/j.issn.2095-3941.2016.0066>
  15. Mehraj U, Dar AH, Wani NA, Mir MA. Tumor microenvironment promotes breast cancer chemoresistance. *Cancer Chemother Pharmacol* **2021**; 87: 147-158. <https://doi.org/10.1007/s00280-020-04222-w>
  16. Mao X, Xu J, Wang W, Liang C, Hua J, Liu J, et al. Crosstalk between cancer-associated fibroblasts and immune cells in the tumor microenvironment: New findings and future perspectives. *Mol Cancer* **2021**; 20: 131. <https://doi.org/10.1186/s12943-021-01428-1>
  17. Bussard KM, Mutkus L, Stumpf K, Gomez-Manzano C, Marini FC. Tumor-associated stromal cells as key contributors to the tumor microenvironment. *Breast Cancer Res* **2016**; 18: 84. <https://doi.org/10.1186/s13058-016-0740-2>
  18. Fozzatti L, Cheng S-y. Tumor cells and cancer-associated fibroblasts: a synergistic crosstalk to promote thyroid cancer. *Endocrinol Metab (Seoul)* **2020**; 35: 673-680. <https://doi.org/10.3803/EnM.2020.401>
  19. Mahauad-Fernandez WD, Okeoma CM. B49, a BST-2-based peptide, inhibits adhesion and growth of breast cancer cells. *Sci Rep* **2018**; 8: 4305. <https://doi.org/10.1038/s41598-018-22364-z>
  20. Roswall P, Bocci M, Bartoschek M, Li H, Kristiansen G, Jansson S, et al. Microenvironmental control of breast cancer subtype elicited through paracrine platelet-derived growth factor-CC signaling. *Nat Med* **2018**; 24: 463-473. <https://doi.org/10.1038/nm.4494>
  21. Huang T-X, Guan X-Y, Fu L. Therapeutic targeting of the crosstalk between cancer-associated fibroblasts and cancer stem cells. *Am J Cancer Res* **2019**; 9: 1889-1904.
  22. Liot S, Balas J, Aubert A, Prigent L, Mercier-Gouy P, Verrier B, et al. Stroma involvement in pancreatic ductal adenocarcinoma: An overview focusing on extracellular matrix proteins. *Front Immunol* **2021**; 12: 612271. <https://doi.org/10.3389/fimmu.2021.612271>
  23. Räsänen K, Virtanen I, Salmenperä P, Grenman R, Vaheri A. Differences in the nemosis response of normal and cancer-associated fibroblasts from patients with oral squamous cell carcinoma. *PLoS One* **2009**; 4: e6879. <https://doi.org/10.1371/journal.pone.0006879>
  24. Pinner S, Sahai E. PDK1 regulates cancer cell motility by antagonizing inhibition of ROCK1 by RhoE. *Nat Cell Biol* **2008**; 10: 127-37. <https://doi.org/10.1038/ncb1675>
  25. Yersal O, Barutca S. Biological subtypes of breast cancer: Prognostic and therapeutic implications. *World J Clin Oncol* **2014**; 5: 412-24. <https://doi.org/10.5306/wjco.v5.i3.412>
  26. Harbeck N, Penault-Llorca F, Cortes J, Gnani M, Houssami N, Poortmans P, et al. Breast cancer. *Nat Rev Dis Primers* **2019**; 5: 66. <https://doi.org/10.1038/s41572-019-0111-2>
  27. Kalluri R. The biology and function of fibroblasts in cancer. *Nat Rev Cancer* **2016**; 16: 582-98. <https://doi.org/10.1038/nrc.2016.73>
  28. Le Clerc J, Tricot-Doleux S, Pellen-Mussi P, Perard M, Jeanne S, Perez F. Expression of factors involved in dental pulp physiopathological processes by nemotic human pulpal fibroblasts. *Int Endod J* **2018**; 51 Suppl 2: e94-e106. <https://doi.org/10.1111/iej.12762>
  29. Granato G, Ruocco MR, Iaccarino A, Masone S, Cali G, Avagliano A, et al. Generation and analysis of spheroids from human primary skin myofibroblasts: an experimental system to study myofibroblasts deactivation. *Cell Death Discov* **2017**; 3: 17038. <https://doi.org/10.1038/cddiscovery.2017.38>
  30. Lappano R, Rigracciolo DC, Belfiore A, Maggolini M, De Francesco EM. Cancer-associated fibroblasts: Role in breast cancer and potential as therapeutic targets. *Expert Opin Ther Targets* **2020**; 24: 559-572. <https://doi.org/10.1080/14728222.2020.1751819>
  31. Broad RV, Jones SJ, Teske MC, Wastall LM, Hanby AM, Thorne JL, et al. Inhibition of interferon-signaling halts cancer-associated fibroblast-dependent protection of breast cancer cells from chemotherapy. *Br J Cancer* **2021**; 124: 1110-1120. <https://doi.org/10.1038/s41416-020-01226-4>
  32. Long X, Xiong W, Zeng X, Qi L, Cai Y, Mo M, et al. Cancer-associated fibroblasts promote cisplatin resistance in bladder cancer cells by increasing IGF-1/ERβ/Bcl-2 signaling. *Cell Death Dis* **2019**; 10: 375. <https://doi.org/10.1038/s41419-019-1581-6>
  33. Hu J, Wang W, Lan X, Zeng Z, Liang Y, Yan Y, et al. CAFs secreted exosomes promote metastasis and chemotherapy resistance by enhancing cell stemness and epithelial-mesenchymal transition in colorectal cancer. *Mol Cancer* **2019**; 18: 91. <https://doi.org/10.1186/s12943-019-1019-x>
  34. Wang H, Wei H, Wang J, Li L, Chen A, Li Z. MicroRNA-181d-5p-containing exosomes derived from CAFs promote EMT by regulating CDX2/HOXA5 in breast cancer. *Mol Ther Nucleic Acids* **2020**; 19: 654-667. <https://doi.org/10.1016/j.omtn.2019.11.024>
  35. Kanyılmaz G, Yavuz BB, Aktan M, Karaağaç M, Uyar M, Findik S. Prognostic importance of Ki-67 in breast cancer and its relationship with other prognostic factors. *Eur J Breast Health* **2019**; 15: 256-261. <https://doi.org/10.5152/ejbh.2019.4778>